# Initiation and suppression of explosive processes in hydrogen-containing mixtures by means of permeable barriers*

*S. V. Khomik,[a,b]* S. P. Medvedev,[a] B. Veyssiere,[b] H. Olivier,[c] O. G. Maksimova,[a] and M. V. Silnikov[a,d]*

[a]*N. N. Semenov Institute of Chemical Physics, Russian Academy of Sciences, 4 ul. Kosygina, 119991 Moscow, Russian Federation. E-mail: khomik@chph.ras.ru*
[b]*Institut PPRIME P´ (UPR 3346 CNRS), Département Fluide-Thermique-Combustion, ENSMA, 1 Avenue Clément Ader, BP 40109, 86961 Futuroscope-Chasseneuil Cedex, France*
[c]*Shock Wave Laboratory, RWTH Aachen University, Templergraben 55, 52056 Aachen, Germany*
[d]*St.-Petersburg State Polytechnical University, 29 ul. Politekhnicheskaya, 195251 St.-Petersburg, Russian Federation. Fax: +7 (812) 552 6080*

Experimental data on the interaction of detonation and shock waves with permeable barriers in cylindrical channels in hydrogen—air mixtures are presented. The method of soot tracks on semi-cylindrical smoked inserts made it possible to elucidate the mechanisms of initiation of the detonation downstream of the barriers. The possibility of initiating explosive processes, including detonation wave decay, is demonstrated. The numerical simulation of the detonation initiation behind the permeable barrier represented by a perforated screen is performed. Analysis of the experimental and calculation results demonstrated that in the near zone behind the barrier, detonation is initiated upon collision (focusing) of hemispherical shock waves emerging from separate holes. In the far zone, the initiation mechanism is similar to that observed on deflagration-to-detonation transition.

**Key words:** detonation, shock wave, initiation, permeable barrier, focusing, hydrogen.

## Introduction

The possibility of formation of large amounts of hydrogen upon nuclear power station accidents as well as the use of hydrogen as a promising fuel in engines and power units bring about the interest in the explosive processes in hydrogen-containing mixtures. The sensitivity to ignition or detonation initiation by an external source is much higher for these mixtures with air than for mixtures of hydrocarbons (except for acetylene) with air. Therefore, hydrogen-containing combustible systems are convenient for experimental research and simulation, in particular, for the cases where permeable barriers are arranged in the propagation path of processes of explosive transition, for example, flame arresters in the channel or barriers or baffles in the room where accident processes arise and develop.

Permeable barriers are modeled using various types of plates mounted across the channel in which the explosive process initiation and development are studied. The plate permeability is provided either by holes, which are most often round or slit-shaped, or by fabrication of the plates from a porous gas-permeable material. If the holes in the plate are round and circularly distributed at various circle diameters, and used in a cylindrical channel, the parameter describing their properties is usually the $Nd^2/D^2$ ratio called open area ratio (OAR), where $N$ is the number of through-holes of diameter $d$ located inside a circle of diameter $D$. If the holes are at the square corners and the distance between their centers is $l$, we get $\mathrm{OAR} = \pi d^2/(4l^2)$. The hole size $d$ is chosen in such a way that the condition $d < \lambda$ holds, where $\lambda$ is the detonation cell width at the initial conditions specified in the experiment.

In typical experimental and simulated setups, a reactive gas mixture, in which some explosive processes can be initiated, is located behind the plate. In this case, ignition of the mixture is also an explosive process, because under certain conditions, the flame can be accelerated, forming destructive compression waves or shock wave (SW) in front of itself. Ahead of the plate, there is a noncombustible inert mixture in which the SW propagates, or a reactive mixture in which the detonation wave propa-

* Based on the materials of the XXV Conference "Modern Chemical Physics" (September 20—October 1, 2013, Tuapse).

Published in Russian in *Izvestiya Akademii Nauk. Seriya Khimicheskaya,* No. 8, pp. 1666—1676, August, 2014.
1066-5285/14/6308-1666 

gates. The detonation initiation or SW formation ahead of the plate are accomplished by standard methods.

The purpose of the work is to arrange systematically the experimental data on the parameters and mechanisms of initiation of explosive processes behind the permeable barrier and analysis of numerical models of the phenomenon.

## Experimental methods

The discrepancies between the experimental studies of different authors are caused by the sort of the permeable plate, the composition of the mixture ahead of and behind the plate, and the type of impact on the plate (detonation wave or SW). Experiments in tubes with internal diameters of 54, 106, and 141 mm were performed.[1—4] Apart from the standard pressure sensors and ionization probes, one of these setups[4] made use of the soot tracks on semi-cylindrical smoked insets of 1 m length. Other researchers used optical recording methods: single-frame schlieren photography,[5] streak recording,[6,7] and inerferometric streak recording.[8]

## Direct initiation of detonation

Figure 1 shows initiation of the detonation directly behind the plate in a tube of diameter 141 mm with the perforated area diameter of 110 mm as the evolution of the overpressure $\Delta P$ profiles measured on the channel wall. In the Figure, the detonation is approaching the plate from the left. It can be seen that at a distance of less than the tube diameter from the plate, the pressure profile is already restored and the velocity becomes equal to the velocity ahead of the plate.

It was suggested[8] for the first time that detonation behind the plate can be initiated upon multi-locus volumetric explosion of a doubly shocked compressed gas behind the shock wave reflected from the plate. In these experiments, detonation was first initiated ahead of the plate and only after that, behind the plate. The mechanism of detonation initiation behind the plate remained unclear. From the experimental data,[7] it was concluded that there is spatial interaction of the compression waves with one another and with the flame front downstream of the plate. However, this process was considered to be the source of turbulence, facilitating degflagration-to-denotation transition (DDT). The interaction of compression waves has not been considered as the source of initiation centers, as these waves were regarded to be weak for the "shock-wave self-ignition" under the experimental conditions.

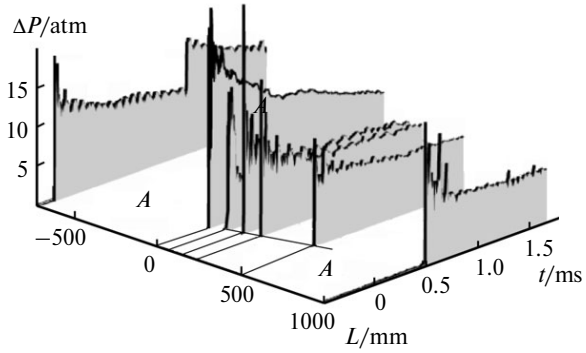


**Fig. 1.** Overpressure $\Delta P$ profiles for detonation and its recovery behind the plate in a $H_2$(30%)+air (70%) mixture at $p_0$ = 1 atm, $d$ = 4.8 mm, OAR = 0.57; the plate is located at $L$ = 0; $A$ is detonation of 1990 m $s^{-1}$.

Consider the scheme of interaction of a shock or detonation wave with a plate having evenly distributed identical holes. Immediately after the start of the reflection from the plate, a SW is formed in each hole, being transformed into a spherical wave after having passed the plate. The interaction of waves that have emerged from neighboring holes results in their 3D-focusing on the axis perpendicular to the plate between the holes. It was found[9] that upon 3D-focusing of SWs having relatively low intensity, a local area functioning as a sort of detonation initiator may appear. If there is only one such area and the energy evolution in it is insufficient for initiation, the SWs propagating from it would be attenuated. However, the presence of a set of such areas in the case of a perforated plate facilitates the detonation initiation. The cause is that, although the energy evolution in each area is insufficient for initiation, the SWs will be enhanced and, after a number of collisions, this will result in initiation of detonation. A similar, but a simpler situation occurs upon the interaction of waves from two parallel slits[10] where focusing is cylindrical, that is, two-dimensional. The soot track of the direct initiation of detonation[4] in a stoichiometric $H_2$—air mixture at $p_0$ = 1 atm, $d$ = 6 mm, and OAR = 0.46 is shown in Fig. 2. The track was obtained using a smoked semi-cylindrical inset. It can be seen that the cellular structure appears at a distance equal to three to five hole diameters and that at distances of 0.3—1.8 tube diameters from the plate, the cell already reaches a size of ~10 mm.

A similar situation occurs when the same plate with OAR = 0.46 and with a separating membrane is used.[11] This soot track is shown in Fig. 3. On the left of the plate there is air at $p_0$ = 0.2 atm over which the plate is approached by an SW with the Mach number $M$ = 5.1. Behind the plate, there is a $H_2$(34%)+air (66%) mixture at the initial pressure $p_0$ = 0.2 atm. After interaction with the plate at a distance of two to four hole diameters, a cellular detonation structure appears and rapidly reaches a steady state.

The performed experiments[4] can serve to establish the domain of initial states and compositions of hydrogen—air mixtures at which the direct detonation initiation is possible. Figure 4 presents the dependence of the initial pressure of the hydrogen—air mixture on the mixture com-

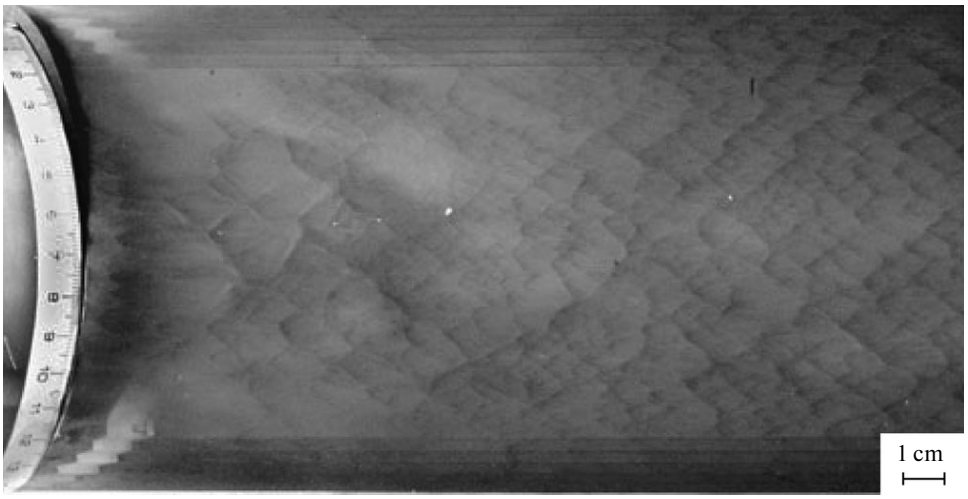


**Fig. 2.** Soot track of direct detonation initiation in a stoichiometric $H_2$—air mixture located on both sides of the plate; the plate is located on the left; the detonation approaches from the left.

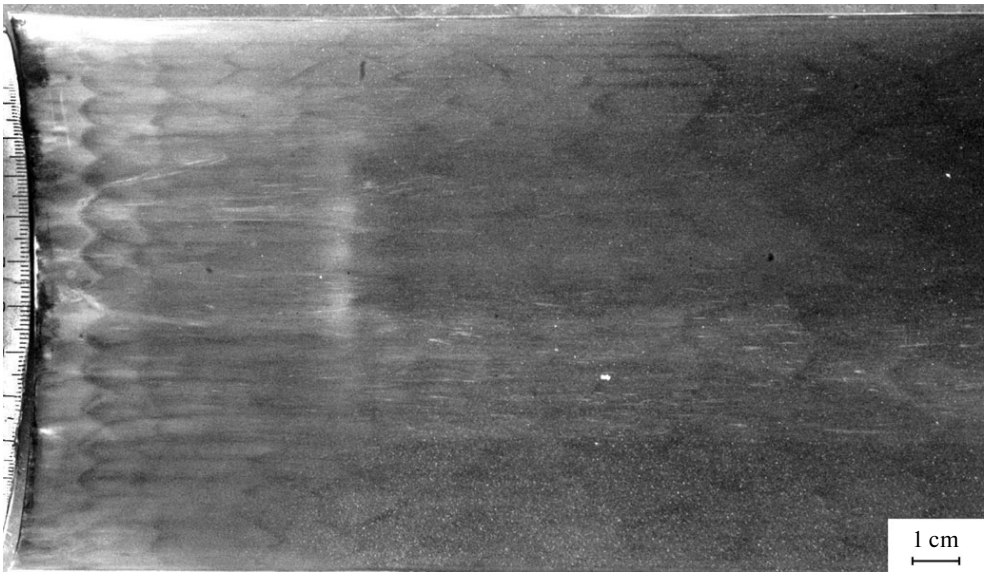


**Fig. 3.** Soot track of direct detonation initiation for air being present upstream (on the left) of the plate and a $H_2$(34%)+air(66%) mixture being present downstream of the plate; the plate is located on the left and is approached by the SW in air from the left.

position for which the detonation is initiated at a length of up to 10 tube diameters. In all cases, the mixture on both sides of the plate was the same and occurred at equal pressures.

The point in Fig. 4 that corresponds to the mixture composition and initial pressure used in the experiment shown in Fig 2 is located deep inside the U-shaped area (see Fig. 4). The dark points present at the boundary correspond to detonation initiation at distances from the plate scaled by the diameter of the tube in which the plate is mounted rather than by the diameter of the hole in the plate. The explosive processes corresponding to this condition are described in the next section.

Measurements of the velocities of explosive processes performed at various distances from the plate provide additional information about the details of the phenomena inside and at the boundary of the U-shaped region. These data are shown in Fig. 5 for various hydrogen and air mixtures in a tube of diameter 141 mm at the initial pressure $p_0$ = 1 atm and OAR = 0.44. These points are located inside the region enclosed by the corresponding curve in Fig 4 and are not shown in Fig. 5.

As can be seen in Fig. 5, only within the initiation limits, i.e., within the U-shaped area, the measured velocities are equal to or lower than the calculated ones. This is due to the fact that the calculation gives thermodynami-

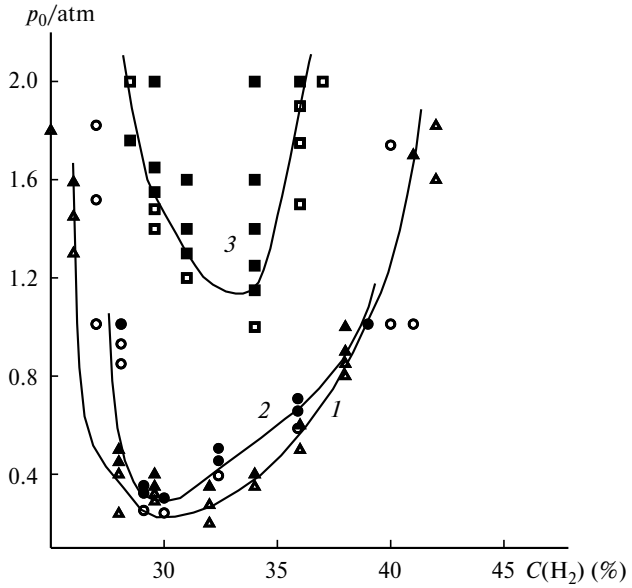


**Fig. 4.** Regions of existence of explosive regimes in the plane initial pressure—hydrogen content in the mixture for various barrier permeability: OAR = 0.46 (*1*), 0.44 (*2*), and 0.42 (*3*); the light dots correspond to the detonation initiation at a distance of <1 m after the plate. The dark dots correspond to the detonation initiation at any distance from the plate. The dots located in the regions enveloped by the U-shaped curves are not shown; $p_0$ is the initial pressure of the reactive mixture upstream and downstream of the plate. The mixture is the same in all cases.

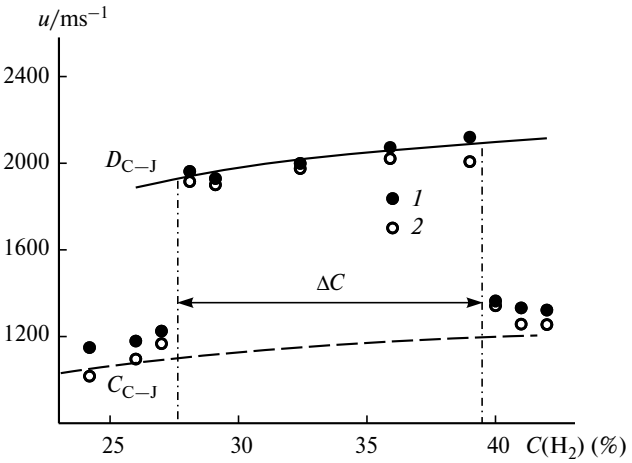


**Fig. 5.** Rate of the explosive process ($u$) at various hydrogen concentrations measured at distances from the plate $x/D_0 = 2.2$ (*1*) and 10.5 (*2*) in a tube of diameter 141 mm; $D_{C-J}$ and $C_{C-J}$ are the calculated values for the Chapman—Jouguet detonation rate and the speed of sound in the combustion products, respectively; $\Delta C$ are the detonation initiation limits at OAR = 0.44.

cally maximum velocities without taking account for the losses. In the vicinity of the inner boundaries and especially outside this region, the velocity is higher near the plate than far from the plate and the difference between them steadily tends to increase, indicating the SW decay. A high velocity near the plate inside the U-shaped region may be indicative of a nonstationary transition process near the boundary of the detonation initiation region, *e.g.*, degflagration-to-denotation transition.

The initiation model proposed in our studies is also supported by the fact that no effect of the mixture composition ahead of the plate on the possibility of detonation initiation behind the plate was found.[12] It was shown that the crucial role is played by the detonation wave intensity ahead of the plate, *i.e.*, the intensity of the SWs that penetrate through the plate.

### Degflagration-to-denotation transition

The energy release upon SW focusing near the obstacle may be insufficient to initiate the detonation directly in this region, which may be caused by both too low intensity of incident SW and low reactivity of the mixture. In these cases, a region arises enclosed by the leading shock front surface on one side and by the surface of the reaction spots (burning front) on the other side. Under appropriate conditions, detonation starts in this region. This regime is called degflagration-to-denotation transition. The experiments performed by the authors reveal the whole sequence of explosion transition regimes downstream of the permeable plate depending on the properties of the mixture and the initial conditions. Figure 6, *a* shows a track obtained in an experiment similar to that presented in Fig. 2 but at lower initial pressure of the mixture: $p_0 = 0.42$ atm.

As compared with the experiment at $p_0 = 1$ atm, here one can note a considerable decrease in the number of initiation centers from which the cellular detonation structure starts to develop. Further pressure decrease, *i.e.*, decrease in the mixture sensitivity, leads to a qualitative change of the track and sharp (up to several channel diameters) increase in the distance from the plate at which detonation is initiated. An example of such process is presented in Fig. 6, *b*. Further decrease in the initial pressure to 0.17 atm results in impossibility of detonation initiation at a distance of less than 1 m from the plate.

When an SW propagating in air hits the plate behind which there is a hydrogen—air mixture, the same trends can be seen. It is sufficient to merely compare the appearance of the track in Fig. 3 with the track (Fig. 7, *a*) obtained for the initial pressure of the mixture increased to 0.6 atm, i.e., at lower intensity of the SW having penetrated through the plate.

Nevertheless, the wave attenuation is still insufficient and the detonation is initiated near the plate, although in a fewer number of points. Further decrease in the intensity of spherical SWs leads to a sharp (up to six channel diameters) increase in the distance to the plate and a qualitative change in the track type. This track for an initial pressure of 1 atm is shown in Fig. 7, *b*.

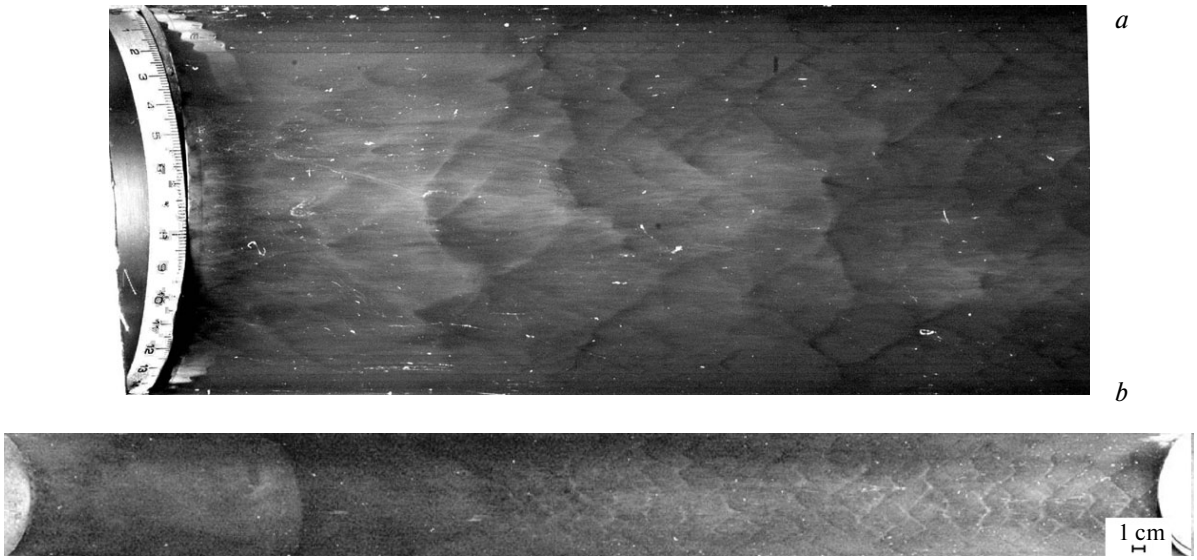


**Fig. 6.** Stoichiometric $H_2$—air mixture on both sides of the plate at $p_0 = 0.42$ (*a*) and 0.2 atm (*b*), $d = 6$ mm and OAR = 0.46; the plate is located on the left and is approached by detonation from the left.

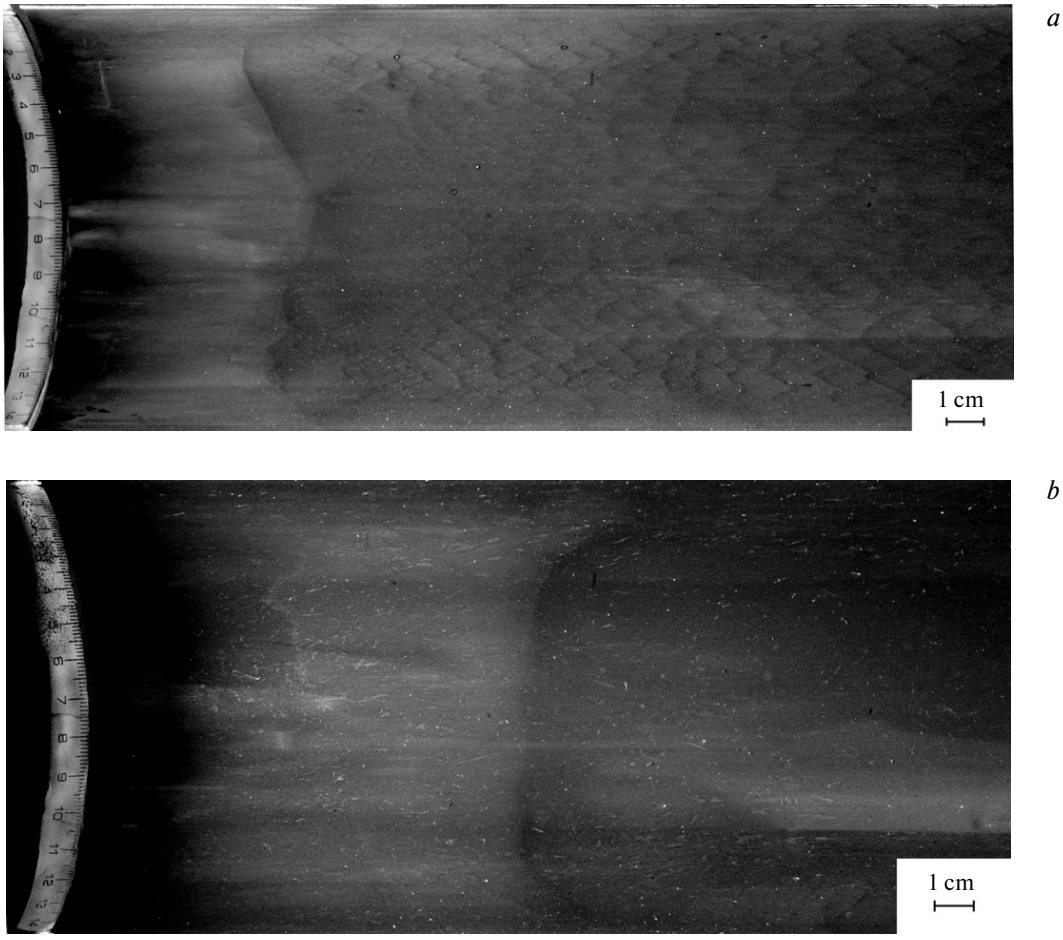


**Fig. 7.** Track obtained under the following conditions: on the left of the plate, air is present at $p_0 = 0.2$ atm; over the air, the SW with the Mach number $M = 5.1$ approaches the plate; behind the plate is the $H_2$(34%)+air(66%) mixture at the initial pressure $p_0 = 0.6$ (*a*) or 1 atm (*b*); the plate is located on the left. The distance from the plate to the "dark" region in Fig. 7, *b* is 6.7 cm.

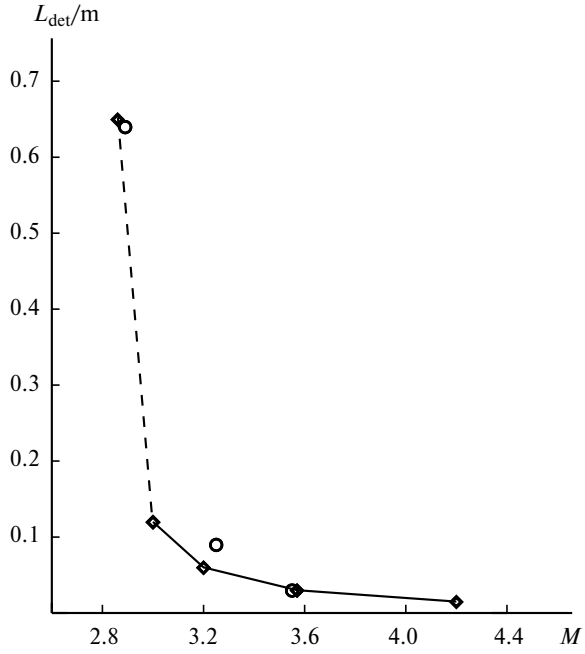


**Fig. 8.** Pre-detonation length ($L_{det}$) *vs.* the Mach number ($M$) of the SW behind the plate. The rhombi correspond to the SW approaching the plate in air with the Mach number $M = 5.1$ for the variable Mach number in a $H_2$(34%)+air(66%) mixture behind the plate as a result of variation of the initial pressure of the mixture. The circles correspond to a constant initial pressure of the hydrogen—air mixture of 0.4 atm (the Mach number of the SW penetrating changes as a result of change in the Mach number of the SW approaching the plate in air).

The dependence of the distance from the plate at which the detonation is initiated ($L_{det}$) on the Mach number $M$ of the shock wave behind the plate is illustrated in Fig. 8. In both cases presented in Fig. 8, one can see a sharp increase in $L_{det}$ upon decrease in the wave intensity in the reactive mixture.

Some publications[5,6] dealing with the interaction of the detonation wave with the plate also noted the deflagration-to-detonation transition regimes. To explain the deflagration-to-detonation transition, it was suggested[5,6] that a one-dimensional turbulent interface between the combustion products and the fresh mixture is formed after the leading SW downstream of the plate. Correspondingly, detonation is initiated by a gradient mechanism[13] upon the turbulent mixing of the fresh mixture with the combustion products. Presented below are the results of author´s calculations demonstrating that the initiation of detonation is possible without resorting to the turbulent mixing concept.

### Quasi-stationary complexes and damping

Apart from the above-considered cases of direct initiation and deflagration-to-detonation transition, it may happen that the detonation wave decays on the plate, and SW and a flame front lagging behind it propagate downstream.[2,3,14] The propagation velocities range over broad limits from 1070 m s$^{-1}$ for the SW and 840 m s$^{-1}$ for the flame (Fig. 9, *a*) to twice lower values observed for the case shown in 9, *b*. In addition, in the latter case, the SW and reaction front (flame) velocities are approximately equal. Hence, the load on the channel walls, as indicated by the pressure profiles shown in 9, *a*, *b*, can differ several-fold in amplitude.

Thus, apart from the regimes resulting in progressing decay and divergence of the SW and flame front, there are regimes resulting in the formation of a quasi-stationary complex consisting of the SW front and the flame front that follows it. As shown in the $L$—$t$ diagrams (Fig. 10), for a perforated plate mounted in a tube of diameter 141 mm with holes located within a circle of diameter 20 mm, the velocity of this complex is ~700 m s$^{-1}$.

In the general case, a complex comprising the SW and the succeeding reaction/flame front is hydrodynamically unstable and may accelerate, which may induce deflagration-to-detonation transition.[8] That is why this complex

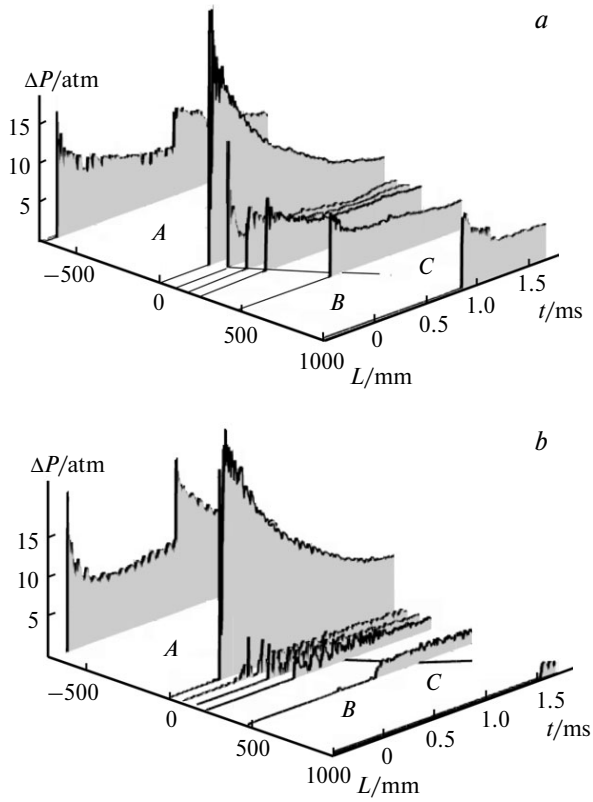


**Fig. 9.** Overpressure $\Delta P$ profiles for detonation ahead of the plate and after detonation decay behind the plate into the SW and the flame front; the plate is located at $L$ = $H_2$(30%) + + air(70%), $p_0 = 1$ atm; (*a*) $d = 3.6$ mm, OAR = 0.43, $D = 110$ mm; $A$ is detonation (1980 m s$^{-1}$), $B$ is SW (1070 m s$^{-1}$), $C$ is flame (1840 m s$^{-1}$); (*b*) $d = 3$ mm, OAR = 0.5, $D = 20$ mm; $A$ is detonation (2020 mm s$^{-1}$), $B$ is SW (650 m s$^{-1}$), $C$ is flame (520 m s$^{-1}$).

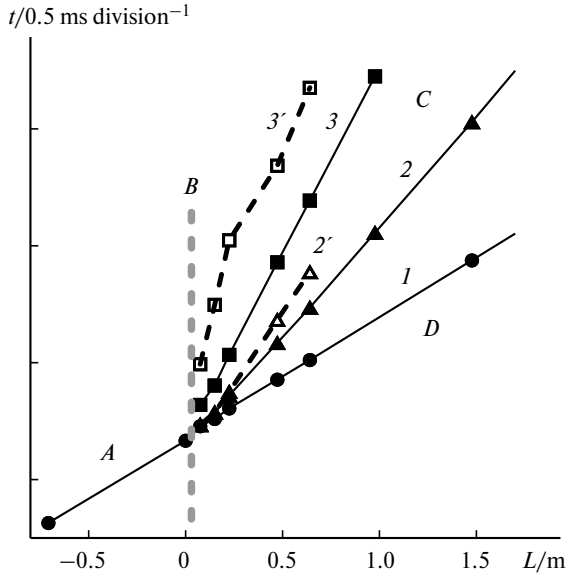


**Fig. 10.** *L*—*t* diagram of the interaction of a detonation wave in a $H_2$(30%)+air(70%) mixture at the initial pressure $p_0$ = 1 atm with various perforated plates. Continuous lines (*1*—*3*) are shock front paths, dashed lines (*2′*, *3′*) are reaction front (flame) paths: *d* = 3.3 mm, OAR = 0.58 (*1*); *d* = 3.6 mm, OAR = 0.43 (*2*, *2′*); *d* = 3.0 mm, OAR = 0.5 (*3*, *3′*); *A* is detonation upstream of the plate, *B* is perforated plate, *C* are SW+flame complexes, *D* is detonation. Diameter of the perforated area is in all cases 110 mm at a tube diameter of 141 mm.

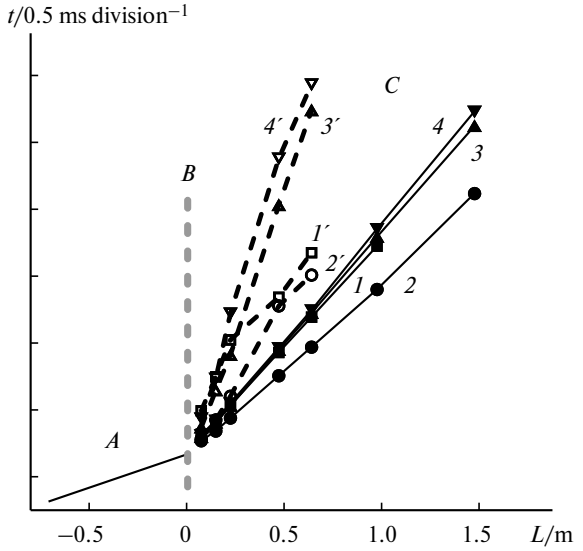


**Fig. 11.** *L*—*t* diagram of the interaction of a detonation wave in a $H_2$(30%)+air(70%) mixture at the initial pressure $p_0$ = 1 atm with various permeable barriers. Continuous lines (*1*—*4*) are shock front paths, dashed lines (*1′*—*4′*) are reaction front (flame) paths; *d* = 3.3 mm, OAR = 0.58, plate diameter 20 mm(*1,1′*); a set of aluminum grids, barrier diameter 110 mm (*2,2′*); metal rubber, barrier diameter 110 mm (*3,3′*); metal wool, barrier diameter 110 mm (*4,4′*); *A* is detonation upstream of the plate, *B* is porous or perforated plate, *C* are SW+flame complexes.

is referred to as quasi-stationary. Unlike the cases reported in the literature, we detected the presence of such complex also downstream of the plate comprising a porous block. Figure 11 shows the *L*—*t* diagrams of explosive regimes resulting from interaction of the detonation wave in a $H_2$ (30%) + air (70%) mixture with various porous materials in a tube of 141 mm diameter at $p_0$ = 1 atm. As these materials, a number of grids, metal wool, and metal rubber were used. The thickness of the porous layer was 16 mm in all cases. The metal wool density was 0.2 g cm$^{-3}$, and the metal rubber density was 2 g cm$^{-3}$.

As can be seen from Fig, 11, the lowest flame propagation velocities are achieved with metal rubber and metal wool plates. In particular, in these cases, the SW velocity decreases to 570—600 m s$^{-1}$ at a flame velocity of up to 200—300 m s$^{-1}$. The distance between the SW and the flame front increases as they move away from the plate up to 0.2—0.3 m for a perforated plate and up to 1.2—1.4 m for the porous metallic materials. Thus, the possibility of increasing the distance between the SW and the flame front to a value of about ten channel diameters was demonstrated. In addition, when a set of aluminum grids is used, as in the case of perforated plate, a quasi-stationary complex is formed at a distance of about four channel diameters from the plate.

The pressure profiles recorded after the plate can be used to compare the ability of various permeable barriers to decrease the intensity of the SW impact on the channel walls. Figure 12 shows these profiles recorded at a distance of 0.2 m after the perforated plate or layers of vari-

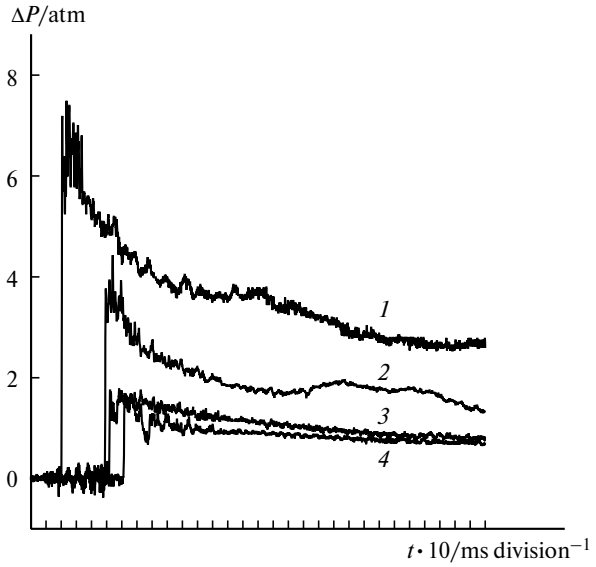


**Fig. 12.** Pressure profiles recorded on the wall of the tube of diameter 141 mm downstream of various barriers approached by detonation of the $H_2$(30%)+air(70%) mixture at the initial pressure of 1 atm: perforated plate, *d* = 3.3 mm, OAR = 0.36 (*1*); set of aluminum grids (*2*); metal rubber (*3*); metal wool (*4*). In the last three cases, the barrier is 16 mm thick.

ous porous materials. It can be seen that blocks of porous materials can decrease the pressure measured at the channel wall ~10-fold. This value is in good agreement with the value found for detonation of a stoichiometric ethylene—air mixture under atmospheric pressure using a standard flame arrester.[15] However, in this case, the flame arrester length was greater than the tube diameter, whereas in our experiment, the plate thickness was related to the tube diameter as ~0.1.

### Formulation of the numerical simulation problem

Experimental elucidation of the details of the detonation initiation process upon the interaction of a detonation or shock wave with a permeable barrier, for example, by the shadow method, is hampered because flowing of the gas out of the barrier holes gives rise to numerous interacting small-scale shock-wave perturbations. Therefore, to study the process details, numerical simulation of regeneration and detonation suppression by the perforated barrier was carried out.[16] The calculations were done using the GasDynamicsTool (GDT) software package[17] in the 3D version for a stoichiometric hydrogen—air mixture.[18] It was found that the detonation initiation just behind the barrier is related to self-ignition in the site of elevated temperature, which arises in the zone of interaction (focusing of the) SW formed during non-stationary jet flow of the detonation products through the barrier perforations.[16] It follows from analysis of the calculation results that the shock-wave mechanism can be applied to description of the detonation initiation and suppression in the near zone downstream of the perforated barrier.

If the combustible mixture fills the space not only behind but also ahead of the barrier, high-temperature reaction products flow through the perforations. A situation is possible that the combustion products are superimposed on self-ignition sites.[16] As a consequence, elucidation of the local conditions resulting in the detonation initiation is hampered. The background effect of the combustion products is eliminated by carrying out calculations for the case in which the plate is hit by the SW propagating in inert gas.[19] In this case, upon SW reflection, inert gas jets move through perforations and form the corresponding hemispherical SW in the reaction medium. The results of numerical simulation[19] confirmed the conclusion that the detonation initiation in the near zone behind the barrier is determined by the self-ignition at high temperature: $T = 1300—1400$ K. Meanwhile, it follows from analysis of experimental data that detonation can also be initiated at considerable distances from the barrier during propagation of the SW—flame front complex. The mechanism of this phenomenon is apparently close to DDT and the characteristic temperatures of the reacting gas are ~1100—1200 K. Thus, in the numerical simulation of the experimentally observed effects, primary attention should be given to the selection of kinetic parameters of ignition in the temperature range $T = 1100—1500$ K. The calculation results that allow one to elucidate the mechanism of detonation initiation both in the near and in the far zone, after the SW has passed though the perforated plate, upon the variation of the kinetic parameters of chemical reaction are presented below.

The calculations were carried out on 3D version by the solution procedure for the Navier—Stokes equation developed in the GDT package and representing modification of the method of coarse particles. It was assumed that the gas is viscous and heat-conductive with the specific heat capacity ratio $\gamma = 1.35$. The chemical reaction rate (one-step mechanism) was described by an Arrhenius type temperature dependence:

$$k = A[\mathrm{F}]^n[\mathrm{O}]^m \exp(-T_a/T), \quad (1)$$

where [F] and [O] are the relative mass concentrations of the fuel and the oxidant (oxygen). As the model reaction system, a stoichiometric hydrogen—carbon oxide (synthesis gas)—air mixture was considered at the volume ratio $H_2 : CO = 1 : 3$. The values $n = 1$, $m = 0.74$ and the heat release of the mixture $Q = 8.9 \cdot 10^6$ J kg$^{-1}$ were constant. The parameter $T_a$ (activation energy) and the factor at the exponent $A$ were varied.

The calculations were carried out for rectangular and non-adaptive grids. One of the perforated barriers used in experiments (thickness $h = 15$ mm, hole diameter $d = 6$ mm) was simulated. The OAR permeability was 0.42. The calculated cell dimension was 0.1 mm. Due to the symmetry condition, the cross-section of the calculation domain was confined by the segment with the dimensions $l/2 \times l/2$; for the chosen parameters, this corresponded to $4.1 \times 4.1$ mm$^2$ (*i.e.*, 1/4 of the hole cross-section was considered, as shown below in the 3D drawings illustrating the calculation results). The length of the calculation domain was up to 420 mm, the maximum number of cells was 7 000 000 at a time step of 10 ns. On the left boundary of the calculation domain, the condition of inert gas inflow with parameters ensuring stepwise pressure and temperature profiles in the incident SW was set.

### Discussion of the numerical simulation results

The procedure of determination of adequate kinetic parameters for simulation of ignition by one-step mechanism requires special consideration. One of the ways is selection of the $T_a$ and $A$ values by comparison with the delay of self-ignition $\tau_{ign}$ calculated in terms of the detailed reaction mechanism. The desired $T_a$ value can be estimated from the relation[20]

$$T_a = \frac{1}{T} \cdot \frac{\mathrm{d}(\ln \tau_{ign})}{\mathrm{d}T^{-1}}. \quad (2)$$

For hydrogen-containing mixtures, the temperature dependence of $\tau_{ign}(T)$ at $p > 0.1$ MPa and $T > 1100$ K has several specific features and cannot be described by a single Arrhenius type equation.[20] Calculations according to the detailed reaction mechanism[21] for the chosen synthesis gas—air mixture demonstrated that for the DDT conditions at $p = 1$ MPa and $T = 1100$—$1500$ K, the effective activation energy values calculated from Eq. (2) vary over a relatively broad range $T_a = 8000$—$34000$ K. For this reason, further verification of the calculation model was performed resorting to experimental data on the initiation of various regimes of explosive transformation with SW focusing in a synthesis gas—air mixture filling a conical deflector mounted at the end of the laboratory shock tube.[9,22] The activation energy values were set to be $T_a = 19000$, 15000, and 11000 K, while the pre-exponential factor was varied. As a result, pairs of parameters were selected, each pair adequately describing the regions of detonation initiation in the synthesis gas with SW focusing: $T_a = 19000$ K and $A = 2.2 \cdot 10^{10}$ s$^{-1}$; $T_a = 15000$ K and $A = 2.7 \cdot 10^{9}$ s$^{-1}$; $T_a = 11000$ K and $A = 2.3 \cdot 10^{8}$ s$^{-1}$. Below, each pair is designated only by the $T_a$ value.

The main series of calculations on the detonation initiation downstream of the perforated barrier was carried out at the invariable Mach number $M = 5.1$ of the incident SW that propagates in air at an initial pressure of 0.2 atm. It was assumed that the barrier is equipped with a membrane that is instantly broken as the SW passes. This made it possible to vary the initial pressure $p_0$ of the combustible mixture downstream of the plate and thus to change the intensity of the SW passed.

The simulated 3D-shots of detonation initiation near the barrier at $p_0 = 0.454$ atm for the case of $T_a = 19000$ K are shown in Fig. 13, *a*. Visualization corresponds to the calculation domain located on the right of the plate. The plate shaped like a segment with dimensions $l/2 \times l/2$ occurs in the left part of the shot. The face located closer to the observer is a symmetry plane between adjacent holes, the upper face is the symmetry plane that passes along the hole axis. The time in microseconds indicated in each

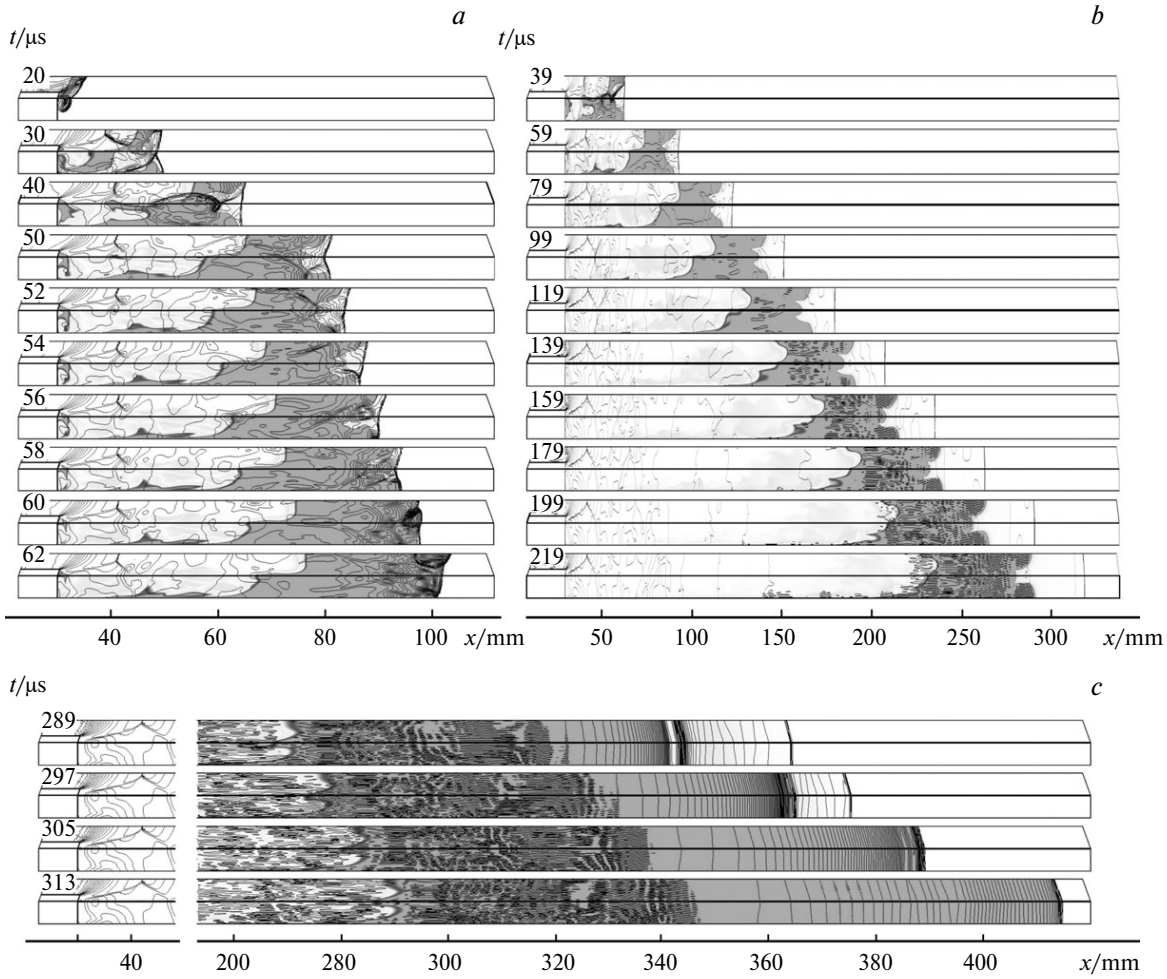


**Fig. 13.** Explosive processes downstream of the perforated barrier at different conditions: (*a*) detonation initiation in the near zone behind the barrier at $T_a = 19000$ K, $p_0 = 0.454$ atm; (*b*) initiation of the SW—reaction front complex at $T_a = 19000$ K, $p_0 = 0.455$ atm; (*c*) detonation initiation in the far zone behind the barrier at $T_a = 11000$ K, $p_0 = 0.71$ atm. For explanations, see the text.

shot is counted from the onset of propagation of the incident SW. The scale of distances has the origin in the left-hand plane of the calculation domain. For the sake of clarity, pressure isolines are presented (every 0.2 atm) with superimposed domains of the dark-gray reaction products.

As can be seen from Fig 13, *a*, the mixture ignites in local spots upon collisions (focusing) of the SWs propagating from adjacent holes. The major self-ignition spot is located on the axis between four neighboring holes (the lower generatrix of each shot). The detonation is initiated upon fast burning-out of the fresh mixture in a lateral pressure wave directly behind the front of the leading SW (shots 58 and 60) at a ~70 mm distance from the barrier. An increase in the initial pressure by only 0.2% to $p_0 = 0.455$ atm sharply changes the flow pattern: detonation is not initiated even at a 400 mm distance from the plate. As can be seen in Fig. 13, *b*, which illustrates this case, the complex consisting of the leading SW and slowing down reaction front is propagating downstream of the plate. In the calculations using $T_a = 15000$ and 11000 K, an increase in the initial pressure does not bring about such a critical phenomenon, *i.e.*, transition to detonation occurs over the whole range of distances upstream of the barrier. An example of detonation initiation in the region at a ~350 mm from the barrier for $T_a = 11000$ K is shown in Fig. 13, *c*. In the considered case, SW is detached in an initial stage from the domain of combustion products. After a certain period of time, the reaction front starts accelerated movement and generates an SW with increasing pressure by the mechanism described previously.[23] In a compressed, nonuniformly heated mixture, a nonstationary explosive wave is generated and overtakes the front of the leading SW (shot 305), thus transforming it into a detonation wave, which propagates further over the quiescent combustible gas at the pressure $p_0$. The elucidated trends are summarized in Fig. 14, which shows the dependences of the detonation initiation distance on the initial pressure.

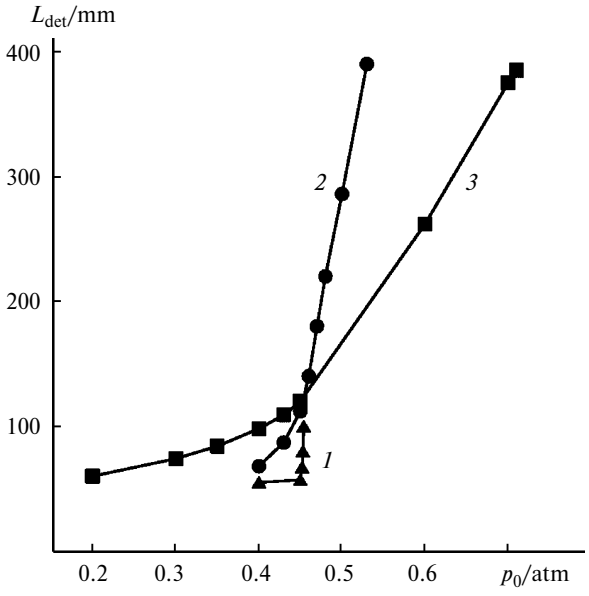


**Fig. 14.** Detonation initiation distance ($L_{det}$) *vs.* initial pressure: $T_a$ =19000 K, $A = 2.2 \cdot 10^{10}$ (*1*); $T_a$ =15000, $A = 2.7 \cdot 10^9$ (*2*); $T_a = 11000$, $A = 2.3 \cdot 10^8$ (*3*).

As can be seen from Figs 13 and 14, two characteristic domains of the detonation initiation parameters can be distinguished. At low initial pressures ($p_0 < 0.454$ atm), detonation is initiated at a distance of up to 70—90 mm from the barrier by the shock-wave self-ignition mechanism upon the collisions of SWs propagating from adjacent holes of the plate. As the initial pressure increases ($p_0 \geq 0.455$ atm), the SW intensity downstream of the barrier is insufficient for direct initiation of the detonation and the SW—reaction front complex is formed. During the propagation of this complex, the reaction front is accelerated and transition to detonation occurs by a mechanism similar to DDT.[23] An important issue is that the behavior of the $L_{det}$—$p_0$ diagrams is determined by the kinetic parameters of the reaction. A decrease in the activation energy extends the range of self-acceleration of the reaction front, which is not observed at all for $T_a = 19000$ K. A probable cause is the high sensitivity of systems with low activation energy to hydrodynamic flow perturbations.

Thus, analysis of the results of numerical simulation sheds light on the mechanism of detonation initiation upon the interaction of shock (detonation) wave with a permeable (perforated) barrier. The characteristic features found in the calculations are in agreement with experimental data and can be used to validate the selection of adequate kinetic parameters of the processes being modeled by comparison with experimental results, in particular, on the distance of the detonation initiation.

This work was financially supported in part by the Russian Foundation for Basic Research (Project No. 12-03-00963-a), Rosatom State Corporation (Contract No. H.4x.44.90.13.1106), and the National Center for Scientific Research (CNRS) of France.

## References

1. S. P. Medvedev, S. V. Khomik, H. Olivier, B. E. Gelfand, in *CD-ROM Proc. Eur. Comb. Meet.*, 2003, Paper 104.
2. S. P. Medvedev, S. V. Khomik, H. Olivier, A. N. Polenov, A. M. Bartenev, B. E. Gelfand, *Shock Waves*, 2005, **14**, No. 3, 193.
3. S. V. Khomik, S. P. Medvedev, B. E. Gelfand, *Comb. Explos. Shock Waves, Int. Ed.*, 2010, **46**, 47 [*Fizika Goreniya i Vzryva*, 2010, **46**, 54].
4. S. V. Khomik, B. Veyssiere, S. P. Medvedev, V. Montassier, H. Olivier, *Shock Waves*, 2012, **22**, No. 1, 199.
5. J.-S. Grondin, J. H. S. Lee, *Shock Waves*, 2010, **20**, No. 5, 381.

6. J. Chao, J. H. S. Lee, in *Proc. of 2002 Spring Technical Meeting*, The Combustion Institute Canadian Section University of Windsor, 2002, Paper 42.1.
7. N. V. Bannikov, A. A. Vasil´ev, *Comb., Explos. Shock Waves, Int. Ed.*, 1992, **28**, 270 [*Fizika Goreniya i Vzryva*, 1992, **28**, 65].
8. R. I. Soloukhin, *Acta Astron.*, 1974, **1**, 249.
9. S. V. Khomik, S. P. Medvedev, A. N. Polenov, B. E. Gelfand, *Comb. Explos. Shock Waves*, *Int. Ed.*, 2007, **43**, 697 [*Fizika Goreniya i Vzryva*, 2007, **43**, 84].
10. T. Obara, J. Sentanuhady, Y. Tsukada, S. Ohya, *Shock Waves*, 2008, **18**, 117.
11. S. V. Khomik, O. G. Maksimova, B. Veyssiere, S. P. Medvedev, *Proc. Int. Coll. on Phys. of Shock Waves, Combustion and Detonation (Minsk, November 14—19, 2011)*, Minsk, 2011, p. 64.
12. S. V. Khomik, B. Veyssiere, S. P. Medvedev, V. Montassier, G. L. Agafonov, M. V. Silnikov, *Shock Waves*, 2013, **23**, No. 3, 207.
13. A. M. Bartenev, B. E. Gelfand, *Prog. Energy Comb. Sci.*, 2000, **26**, 29.
14. S. V. Khomik, B. Veyssiere, S. P. Medvedev, V. Montassier, H. Olivier, in *Nonequilibrium Phenomena: Plasma, Combustion, Atmosphere*, Eds G. D. Roy, S. M. Frolov, A. M. Starik, Torus Press Ltd., Moscow, 2009.
15. G. Thomas, *Proc. Symp On Shock Wave*, ISAS, SAGAMIHARA, KANAGAVA, Japan, 2001, p. 589—592.
16. S. P. Medvedev, S. V. Khomik, B. E. Gelfand, *Russ. J. Phys. Chem. B* (*Engl. Transl.*), 2009, **3**, 963 [*Khim. Fiz.*, 2009, **28**, No. 12, 52].
17. A. V. Zibarov, D. M. Babaev, A. M. Shadskii, *SAPR i grafika* [*CAD and Graphics*], 2000, **10**, 44 (in Russian).
18. N. M. Marinov, C. K. Westbrook, W. J. Pitz, in *Transport Phenomena in Combustion*, Ed. S. H. Chan, **1**, Taylor and Francis, Washington (DC), 1996, p. 118.
19. O. G. Maksimova, S. P. Medvedev, S. V. Khomik, G. L. Agafonov, in *Gorenie i Vzryv* [*Combusion and Explosion*], Ed. S. M. Frolov, Torus Press, Moscow, 2012, p. 125 (in Russian).
20. B. D. Taylor, D. A. Kessler, V. N. Gamezo, E. S. Oran, *Proc. Comb. Institute,* 2013, **34**, 2009.
21. A. Y. Kusharin, G. L. Agafonov, O. E. Popov, B. E. Gelfand, *Comb. Sci. Technol.*, 1998, **135**, 85.
22. O. G. Maksimova, S. P. Medvedev, S. V. Khomik, G. L. Agafonov, *Conference "Khimicheskaya Fizika i Stroenie Veshchestva: k 90-Letiyu So Dnya Rozhdeniya V. I. Gol´danskogo"* [*Chemical Physics and Structure of Matter Dedicated to the 90th Anniversary of V. I. Gol´dansky birth*], *Abstrs.*, Torus Press, Moscow, 2013, p. 56 (in Russian).
23. M. F. Ivanov, A. D. Kiverin, M. A. Liberman, V. E. Fortov, *Dokl. Phys.* (*Engl. Transl.*), 2010, **55**, 480 [ *Dokl. AN*, 2010, **434**, 756].

*Received February 3, 2014*